



Preparation of amine or carboxyl groups modified cellulose beads for removal of uranium (VI) ions from aqueous solutions

Gulay Bayramoglu · Serhad Tilki ·
Mehmet Yakup Arica

Received: 7 June 2023 / Accepted: 11 April 2024
© The Author(s) 2024

Abstract In the present study, cellulose beads were prepared using the phase inversion method and then activated with epichlorohydrin. The epoxy groups of the activated beads were modified with $N\alpha,N\alpha$ -bis(carboxymethyl)-L-lysine hydrate (CML), and tetraethylenepentamine (TEPA) ligands. These modified beads, coded as cellulose-COOH and cellulose-NH₂, respectively, were used to remove of uranium (VI) ions from aqueous medium. The prepared adsorbents were characterized using FTIR, SEM, zeta-potential, and analytical methods; the performance of both the modified beads for the removal of uranium (VI) ions was optimized using different operational parameters in a batch system. The amount of adsorbed uranium ions on cellulose-COOH and cellulose-NH₂ beads was 462.9 ± 13.7

and 127.4 ± 5.1 mg/g, respectively. The results are acceptable regarding the equilibrium kinetics for the adsorption of uranium (VI) ions, which followed the second-order kinetic model. The prepared activated cellulose beads could be utilized in many technological applications by making appropriate modifications in the reactive epoxy groups of cellulose.

Keywords Uranium (VI) removal · Cellulose beads · Polycationic and polyanionic groups · Adsorption · Kinetics

Introduction

Nowadays, nuclear energy has gained significance worldwide due to the fast increase in worldwide energy requests and the pursuit of minimizing environmental pollution without carbon emissions and reliable energy sources (Ahmed et al. 2021; Bai et al. 2022). Uranium is a highly hazardous rare element in the manufacturing nuclear energy and is frequently found in the environment in uranium (VI) form (Bi et al. 2021; Celikbicak et al. 2021). However, uranium is highly toxic to living things. For humans, it affects several organs, such as kidneys, lungs, and livers (Cheng et al. 2021; He et al. 2022). According to the WHO proposal, the maximum limit of uranium in water for human health should be less than 15 µg/L (WHO 2011). Therefore, effective methods are needed for the removal of uranium (VI) ions from

Supplementary Information The online version contains supplementary material available at <https://doi.org/10.1007/s10570-024-05909-6>.

G. Bayramoglu (✉) · S. Tilki · M. Y. Arica
Biochemical Processing and Biomaterial Research
Laboratory, Gazi University, Teknikokullar, 06500 Ankara,
Turkey
e-mail: g_bayramoglu@hotmail.com

G. Bayramoglu
Department of Chemistry, Faculty of Sciences, Gazi
University, Teknikokullar, 06500 Ankara, Turkey

S. Tilki
Department of Chemistry, Sciences and Arts Faculty,
Amasya University, 05100 Amasya, Turkey

aqueous solutions. Various techniques have been developed and used to reduce the uranium contents of the solutions. Presently, the removal techniques of uranium from water are adsorption, chemical precipitation, solvent extraction etc. (Xiao et al. 2021; Singh et al. 2022). Among them, the adsorption method was generally used for the removal of inorganic and organic pollutants from water due to the low cost of many different adsorbents, easy operation, and high efficacy method (Bayramoglu and Arica 2019; Bayramoglu and Arica 2017; Chen et al. 2023; Deng et al. 2021, Huang et al. 2021). In previous years, various microbial biomasses (Bayramoglu et al. 2018; Bayramoglu et al. 2015; Fan et al. 2021; Smjecanin, et al. 2022), hydroxyapatite-biochar nanocomposite (Ahmed et al. 2021; Chen et al. 2023), modified silica particles (Bayramoglu and Arica 2019; Hamza et al. 2022), polymeric beads (Bayramoglu and Arica 2017), amidoximated adsorbents (Bi et al. 2021; Zhang et al. 2023; Zhou et al. 2021; Ashrafi and Firouzzare 2021; Xiao et al. 2021), magnetic adsorbents, carboxymethyl cellulose supported magnetic graphene oxide composites (Zong et al. 2019), composite membrane (Orabi et al. 2021), chitosan modified TiO₂ (Wang et al. 2020), amidoxime functionalized chitosan (Zhu et al. 2023) and various materials have been extensively employed to remove uranium from wastewater using the adsorption technique (Liu et al. 2022; Liu et al. 2021; Minrui et al. 2022; Peng et al. 2023). On the other hand, it needs to develop new adsorbents that are inexpensive, easy to prepare, with high durability, and high adsorption capacity under diverse experimental conditions. Furthermore, they should be easily separated from the adsorption medium and without generating secondary pollutants. Adsorbents with amine or carboxyl groups for rapid adsorption processes have gained importance in terms of the functionalization of materials for the removal of metal ions from wastewater due to the easy interaction of metal ions with these groups. Therefore, for the design new adsorbents the solid supports have been mostly modified with amine or carboxyl groups by the researches (Arica and Bayramoglu 2016; Orabi et al. 2021). For examples, Shen et al. (2022) prepared a porous polyethylenimine-carboxylated chitosan / oxidized charcoal composite to remove uranium ions, the adsorption process was very rapid with this polyamine modified adsorbent for uranium ions. Xiao et al. (2021) functionalized luffa fiber with carboxyl

and amidoxime groups for the removal of uranium (VI) ions from mine water, and these groups showed high adsorption capacities for uranyl ions. Generally, ligand molecules are not used directly as an adsorbent due to their small sizes and high water solubilities. Therefore, they are immobilized on a solid support to obtain high capacity functional adsorbents. The preparation and design of novel adsorbents from natural polymeric materials are very important due to their large quantity availability in nature and also biodegradable without the production of secondary pollutants in the environment (Arica et al. 2022).

Cellulose is the major natural polymer in the environment. Moreover, cellulose is an inexpensive natural polysaccharide with reach pendant hydroxyl groups. These groups could be easily modified with various ligands to prepare a high performance adsorbent. The modified cellulose based materials can form chelate or complex with metal ions and/or other organic pollutants. On the other hand, the low mechanical strength and poor thermal stability of cellulose-based adsorbents may limit their application in the adsorption method. Crosslinking cellulose based materials with various crosslinking agents may improve their mechanical properties and large scale applications (Gericke, et al. 2013). As reported in earlier studies, cellulose is an excellent material for preparing sustainable adsorbents due to its easy obtainability, renewability, and biodegradability. Cellulose is a linear polymer composed of β -1–4-linked D-glucopyranose repeating units (French 2017; Hana et al. 2013). It has many useful properties for use in the area of biotechnology as a natural renewable polymeric materials (Edwards et al. 2012; Bayramoglu et al. 2023). The available hydroxy groups of cellulose are easily modified by reacting with various ligand molecules, and a wide range of cellulose derivatives could be obtained.

In the presented work, cellulose-based cross-linked adsorbent was prepared and modified with two different ligands Na,N α -bis(carboxymethyl)-L-lysine or/and tetraethylenepentamine, which can affect the adsorption performance of the target metal ions. The as-prepared cellulose-based adsorbents with different functionalities were evaluated for the removal of uranium (VI) ions from the aqueous solution.

To the best of our knowledge, this work is the first report for preparing polyanionic and polycationic cellulose beads for the adsorption of uranium (VI) from

the solution. The cellulose beads were prepared via the phase inversion method and cross-linked/activated with epichlorohydrin. Next, the free amino groups of Na,N α -bis(carboxymethyl)-L-lysine or tetraethylenepentamine ligands were reacted with the epoxy groups of epichlorohydrin to synthesize polyanionic and polycationic adsorbents named cellulose-COOH and cellulose-NH₂, respectively. Adsorption isotherms and kinetics models were applied to experimental data to assess the effect of polyanionic and polycationic groups of the adsorbents while interacting with uranium (VI) ions. The adsorption mechanism of uranium (VI) on both adsorbents and the effect of functional groups on adsorption processes were evaluated.

Materials and methods

Materials

Microcrystalline cellulose (20–160 μ m), 1-Ethyl-3-methylimidazolium acetate (EMIM-Ac,

C₈H₁₄N₂O₂), dimethyl sulfoxide (DMSO), N α ,N α -bis(carboxymethyl)-L-lysine hydrate (CML, C₁₀H₁₈N₂O₆·xH₂O), tetraethylenepentamine (TEPA, H₂N-(CH₂)₂-NH-(CH₂)₂-NH-(CH₂)₂-NH-(CH₂)₂-NH₂), and epichlorohydrin were obtained from Sigma-Aldrich (Hamburg, Germany). Uranyl acetate was supplied from Honeywell Riedel-de-Haën AG (Germany), and uranium (VI) solutions were prepared from (UO₂(CH₃COO)₂·2H₂O) in deionized water. Diethylenetriamine pentaacetic acid (DTPA), sodium hydroxide, hydrochloric acid, and arsenazo (III) (1,8-dihydroxynaphthalene-3,6-disulfonic acid-2,7-bis[(azo-2)-phenylarsonic acid) were supplied from Sigma-Aldrich. All these chemicals were used as received in the experimental work.

Preparation of amine or carboxyl groups modified cellulose beads

The preparation of amine or carboxyl groups modified cellulose beads was realized in two sequential steps (Fig. 1). Firstly, pristine cellulose beads were prepared via the phase inversion method. Microcrystalline cellulose (4.0 g) and DMSO (40 mL) were transferred in a three-necked reaction vessel and equipped with an overhead stirrer. Then, 16.5 g of

1-ethyl-3-methylimidazoliumacetate was added drop by drop in the reaction vessel, stirred at room temperature, and at 750 rpm for 5.0 h. After this period, the cellulose solution was dropped into pure ethanol using a syringe pump at a fixed flow rate through an injection needle (diameter 1.0 mm). The formed cellulose beads were stirred to avoid aggregation in pure ethanol at 200 rpm for 90 min. This process further furnished the stability of the formed bead structure. Then, the beads were collected by filtration, transferred to a three-necked reaction vessel containing pure ethanol, and refluxed for 24 h at 80 °C to remove any remaining DMSO and EMIM-Ac.

Then, the reaction temperature was raised to 65 °C and stirred for 3.0 h. Later, the activated cellulose beads were collected and washed twice with deionized water and 70% ethanol, respectively.

Then, the beads were incubated in deionized water with two fresh exchanges for 24 h. After these processes, the prepared cellulose beads had a spherical morphology and a narrow size distribution (approximately 0.95 \pm 0.09 mm). For the activation reaction, the as-prepared cellulose beads (5.0 g) and NaCl (1.0 g) were added into NaOH solution (50 mL, 10%, w/w), and stirred at room temperature for 15 min. After that, 5.0 mL of epichlorohydrin was introduced dropwise to this mixture within 10 min, and the reaction temperature was raised to 65 °C and stirred for 3.0 h. The activated cross-linked cellulose beads were filtrated, and washed twice with deionized water and 70% ethanol. Some of the activated cellulose beads were transferred into N α ,N α -bis(carboxymethyl)-L-lysine hydrate or/and tetraethylenepentamine solution (50 mL, 50 mg CML or/and TEPA), and the pH of the solution was adjusted to 9.0 using 0.1 mol/L NaOH solution. Binding reactions of CML and TEPA ligands onto activated cross-linked cellulose beads were carried out at 65 °C for 8.0 h. After the reaction, the cellulose beads modified with CML or TEPA ligands were collected by filtration. Physically bound ligands were removed by washing with saline solution (100 mL, 0.5 mol/L NaCl) and with dilute HCl solution (pH 5.0, 100 mmol/L) in the given order. The cellulose beads modified with CML or/and TEPA ligands were coded as cellulose-COOH and cellulose-NH₂ beads. Bare cellulose beads were prepared by continuously mixing epichlorohydrin-activated cellulose beads in H₂SO₄ solution (0.5 mol/L, 50 mL) at 50 °C for 2.0 h and used as a control. During this

reaction, the epoxy groups of the cellulose beads were converted into hydroxyl groups. Then, the beads were washed with purified water and dried at room temperature for 24 h. The modified cellulose beads were stored at 4 °C until use. A schematic representation of the preparation of adsorbents is presented in Fig. 1.

Characterization of the as-prepared cellulose beads

The amounts of free carboxyl and amino group content of the cellulose-COOH and cellulose-NH₂ beads were detected using potentiometric titration as described previously (Celikbicak et al. 2021). The surface morphology of the cellulose beads was obtained by scanning electron microscopy (SEM, FEI QUANTA 250 FEG, Oregon, US). The properties of the materials were studied with an FTIR spectrometer (Nicolet TM ISTM 50, Thermo Fisher Scientific,

USA). The zeta potential values of the cellulose-OH, cellulose-NH₂, and cellulose-COOH beads were obtained at various pH values and analyzed using a Zeta-sizer (Nano ZS, Malvern Instruments Ltd., Model number: ZEN3600). The specific surface areas of cellulose-OH, cellulose-NH₂, and cellulose-COOH were determined by a surface area device (Quantachrome Nova 2200 E, USA) and calculated using the Brunauer–Emmett–Teller (BET) method (Brunauer et al. 1938). The water content of the cellulose bead preparations was determined by a gravimetric method. The dry and wet masses of the cellulose beads samples (d_m and w_m , respectively) were weighed, and the samples were added to deionized water at room temperature for 12 h. The water content of the cellulose bead samples was calculated as:

$$\text{Equilibrium water content (\%)} = [(w_m - d_m)/d_m] \times 100 \quad (1)$$

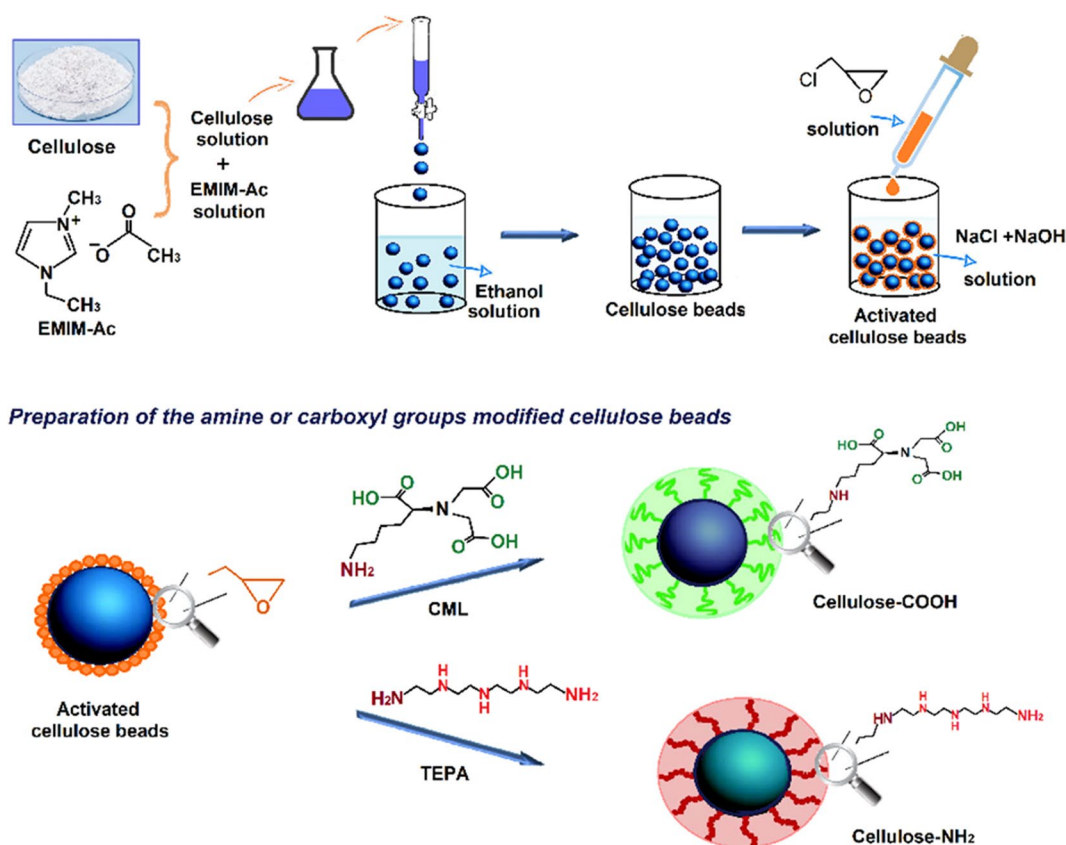


Fig. 1 Schematic representation of the preparation of the adsorbents

Uranium (VI) ion adsorption from the aqueous solution

The adsorption of uranium (VI) ions with the cellulose-COOH and cellulose-NH₂ beads was performed in a batch system using cellulose-OH as a control system. Varying amounts of uranium solutions were prepared from a stock solution of 1000 mg uranium / L in deionized water. Adsorption studies were performed using adsorbent samples (10 mg) in 20 mL of uranium (VI) solution (100 mg/L) at 25 °C for 180 min. The effects of pH and salt concentration on uranium (VI) adsorption efficiency were investigated at NaCl concentrations varying between pH 3.0 and 8.0 and 0.0–1.0 mol/L, respectively. The influence of adsorbent dose was studied by changing the amount of the adsorbent in solution (0.1–1.25 g/L). The effect of temperature was studied at four different temperatures (i.e., 15, 25, 35, and 45 °C). The initial concentration of U(VI) ions was varied in the range of 10–300 mg/L. Spectrophotometric determination of uranium (VI) ions was realized using the arsenazo (III) method as described earlier (Celikbicak et al. 2021). Briefly, arsenazo III solution was prepared by dissolving 0.25 g of arsenazo (III) in NaOH solution (50 mM, 100 mL). A known amount of uranium solution and DTPA solution as a complexing agent (2.0 mL, 2.5%) and 1.0 mL of arsenazo (III) solution were added, and the rest of the volume was completed to 50 mL with H₂SO₄ solution (pH 2.0). After 3 min, the pink-violet color was measured at 651 nm using a double beam UV/vis spectrophotometer (PG Instrument Ltd., Model T80+; PRC) as mentioned in a report published work (Celikbicak et al. 2021).

Repeated use studies

The repeated adsorption/desorption experiments were studied using 10 mg cellulose-NH₂ or cellulose-COOH beads in a 20 mL uranium (VI) solution

(100 mg/L) at 25 °C for 180 min. For desorption, cellulose-NH₂ or cellulose-COOH beads were eluted using HNO₃ (20 mmol/L) solution. The adsorbents were transferred in a desorption medium and stirred for 180 min. The adsorbents were transferred to fresh uranium (VI) solution and mixed for 180 min for each repeated use experiment. These cycles were repeated seven times with the same adsorbents. The amount of uranium (VI) in the solution was determined as described above.

Statistical studies

All the experiments were repeated at least three times, and average values were used in material preparation and uranium (IV) adsorption studies. These data were expressed as mean values ± standard deviation (SD). The statistical analyses were evaluated using one-way analysis of variance (ANOVA) on Origin Pro 9 software. The significant difference among the average was realized through a paired comparison test with $p < 0.05$.

Results and discussion

Properties of the modified cellulose-based adsorbents

The cellulose beads were prepared via the phase inversion method and crosslinked/activated with epichlorohydrin (with a diameter of around 2.0 mm). CML and TEPA ligands were then immobilized onto activated cellulose beads by reacting amino groups with epoxy groups. The amounts of carboxyl and amine groups were determined as described above, and the amount of available carboxyl and amine groups of the cellulose-COOH and cellulose-NH₂ were presented in Table 1. Some activated beads were hydrolyzed with H₂SO₄, and these -OH groups were used as a control system in the adsorption studies.

Table 1 Functional group and water contents of the as-prepared cellulose bead preparations

	Epoxy groups (mmol/g)	Carboxyl groups Theoretical/Experimental (mmol/g)	Amine groups	Water (%)
Activated cellulose beads	32.4 ± 1.3	-	-	87.3 ± 4.1
Cellulose-COOH	-	97.2/78.7 ± 3.6	-	96.2 ± 3.7
Cellulose-NH ₂	-	-	162.0/86.9 ± 3.9	92.5 ± 4.8

The acid hydrolyzed beads were denoted as cellulose-OH. The water contents of the cellulose based beads preparations are presented in Table 1. As observed from the table, the water content of the ligand-immobilized cellulose beads increased compared to the bare cross-linked cellulose beads (cellulose-OH). The CML and TEPA ligands are rich in carboxyl and amine groups, respectively, and they are highly hydrophilic and easily soluble in aqueous media. Therefore, the water contents observed for the CMC and TEPA ligand-immobilized cross-linked cellulose beads were higher than the bare cross-linked cellulose beads. The specific surface areas of the prepared cellulose-OH, cellulose-NH₂, and cellulose-COOH were measured by the BET method and found to be 20.7, 17.8, and 19.1 m²/g, respectively. After modification reactions with N_α,N_α-bis(carboxymethyl)-L-lysine, and tetraethylenepentamine, the surface area of cellulose-NH₂ and cellulose-COOH reduced by about 14.0 and 7.7%, respectively, compared to cellulose-OH. These observed reductions in the surface area of the cellulose-NH₂ and cellulose-COOH could be due to the filling of the vicinity of pores with the immobilization of CMC or TEPA ligands. The reduction was more pronounced for the -NH₂ modified cellulose beads. This could be the result of the hydrogen bonding interactions between -OH groups of the cellulose and amine groups of N_α,N_α-bis(carboxymethyl)-L-lysine ligand.

The crosslinked cellulose bead surface micrographs were examined using scanning electron microscopy (SEM). The SEM image of the activated cellulose beads with a larger population is also presented in Fig. S1. These SEM images can provide information on the beads in size, shape, and surface morphology. The surface of the activated cellulose bead with high magnification is also shown in Fig. 2. As exemplified in Fig. 2A, they had rough surfaces and were mainly spherical in shape. As observed at the high magnification, the cellulose beads had a highly porous structure (Fig. 2B). These pores provide a large surface area, and the overall increased surface area considerably enhances the contact surfaces with uranium ions in the solution.

The functional groups on the modified cellulose-based adsorbents can be dissociated according to the medium pH (Fig. 3). The zeta potential plot for the cellulose-OH, cellulose-COOH, and cellulose-NH₂ showed different surface properties as experimented

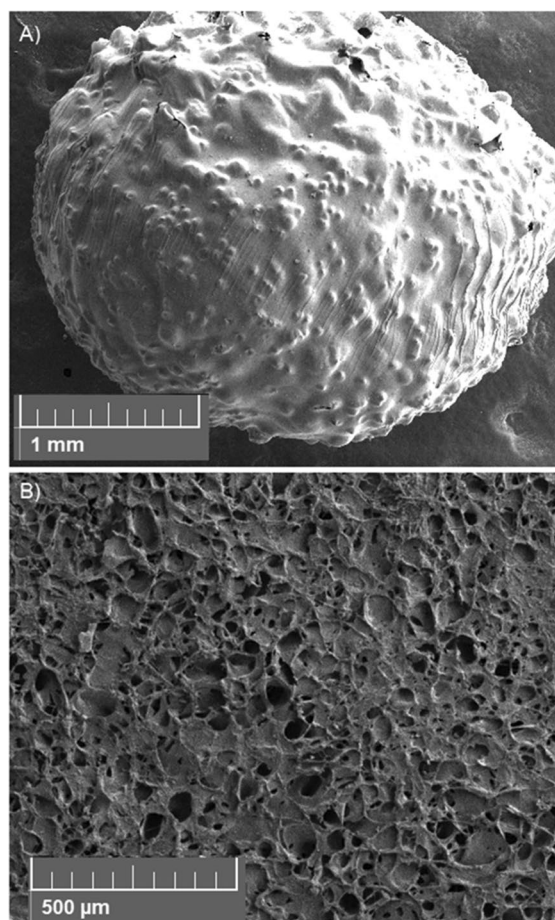


Fig. 2 SEM micrographs: **A** Crosslinked cellulose X40; **B** Surface of crosslinked cellulose beads X200

with in other studies (Bayramoglu et al. 2018). The zeta potential values of the cellulose-OH and cellulose-COOH decreased as the medium pH increased. As seen in this figure, the negative charge density of the cellulose-COOH was higher than the cellulose-OH. The charge densities of the cellulose-OH and cellulose-COOH in the pH range 2.0–11 changed between -3.4 and -16.1, and -22.4 and -57.5 mV, respectively. On the other hand, in the studied pH range, the surface potentials of cellulose-NH₂ were observed to be positive. A positive zeta potential value for cellulose-NH₂ resulted from incorporating the positively charged amine groups. The charge densities of the cellulose-NH₂ in the pH range of 2.0–11.0 changed between 35.1 and 55.2 mV. Thus, the difference in the zeta-potential values confirmed the effectiveness of the functionalization of

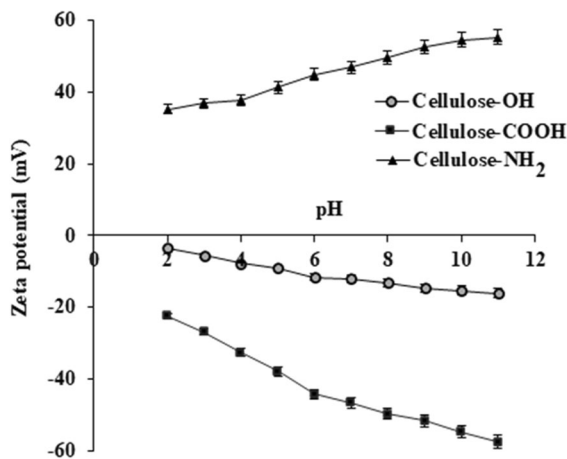


Fig. 3 The zeta potentials data of the (A) cellulose-OH, B cellulose-NH₂, and (C) cellulose-COOH as a function of medium pH. Zeta potential measurements were achieved in each condition as three measurements. The replicates were done to achieve a reliable data basis for values

the cellulose bead's surface with amine or carboxyl groups. It should be noted that the cellulose-COOH and cellulose-NH₂ adsorbents were highly stable at the studied pH values. No aggregations were observed for both modified cellulose beads under given experimental conditions.

The ATR-FTIR spectra of the cellulose-OH, cellulose-COOH, and cellulose-NH₂ are presented in Fig. 4. For the cellulose-OH beads a broad band was observed at 3346 cm⁻¹ due to the -OH stretching vibration of hydroxyl groups (Fig. 4A). The bands for pure cellulose at 2998 and 1659 cm⁻¹ could be assigned for C-H and C-C stretching and vibration, respectively. The peak at 1057 cm⁻¹ was observed for -C-O- skeletal vibration of cellulose. The FTIR spectrum of the cellulose-NH₂ preparation is presented in Fig. 4B.

The results showed that the wide absorption band at 3374 cm⁻¹ could be ascribed to the stretching vibration of -OH and primary and secondary amine groups of TEPA ligand immobilized on the cellulose beads. The presence of the -NH-CO- and -C-N- peaks at 1649 cm⁻¹ and 1582 cm⁻¹ in the cellulose-NH₂ spectrum confirmed the immobilization of the TEPA ligand onto the cellulose structure. After attachment of *N*_ω*N*_α-bis(carboxymethyl)-L-lysine ligand (i.e., cellulose-COOH) on the cellulose beads, the -OH group band of cellulose was noticed

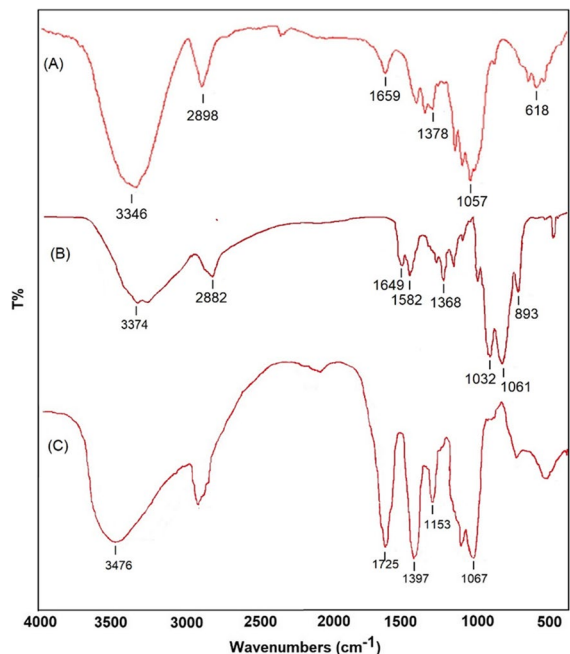


Fig. 4 ATR-FTIR spectra: A cellulose-OH, B cellulose-NH₂ and (C) cellulose-COOH

at 3476 cm⁻¹ (Fig. 4C). In the cellulose-COOH spectrum, the typical peak recorded at 1725 cm⁻¹ could be about the stretching vibration of C=O in -COOH, and this peak confirmed the successful immobilization of the CML ligand on the cellulose beads. The symmetrical stretching vibrations of -COO- happened at 1396 cm⁻¹. The stretching vibration peaks of C-O-C and C-OH were detected at 1153 and 1067 cm⁻¹, respectively. All these observed changes were correlated with the immobilization of both ligands on the activated cellulose beads.

Adsorption studies

Influence of adsorbent dosage and ionic strength on the removal efficiencies

The adsorbent dosage is one of the critical limitations for the adsorption of uranium (VI) ions on the cellulose-NH₂ and cellulose-COOH beads. The effect of adsorbent dosage on the removal efficiency was studied by changing the rate between 0.1 and 1.25 g adsorbent/L (Fig. 5). As shown in this figure, an increase in the percent removal of uranium (VI) ions was detected about the increase in the adsorbent

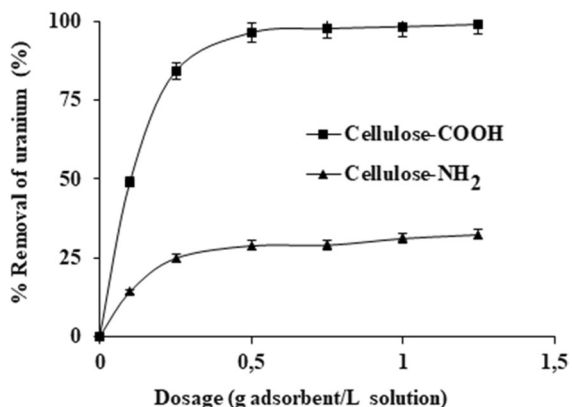


Fig. 5 Adsorbent dosage on the adsorption performance of uranium (VI) on the cellulose-NH₂ and cellulose-COOH. (Initial concentration of the uranium ions, 100 mg/L; temperature, 25 °C; contact time, 120 min; stirring rate, 150 rpm)

dosage. This increase in the adsorption performance of the uranium (VI) ions can result from the increase quantity of accessible binding sites with the increasing amount of adsorbent in the solution. On the other hand, the amount of removed uranium (VI) ions per unit mass of the used adsorbents decreased reliably with the increased amount of the adsorbent preparations. The reduction in adsorption capacities of the used adsorbents can be due to the adsorptive sites of the adsorbent not fully occupied with the uranium (VI) ions. The removal performance of uranium (VI) ions of the adsorbents in order was cellulose-COOH > cellulose-NH₂. Since the optimum adsorption dose was around 0.5 g/L adsorbent, this dosage was used for the remaining studies.

The effect of salt concentration on the adsorption of uranium (VI) ions on the cellulose-COOH and cellulose-NH₂ was studied by varying salt concentration in the solution (Fig. 6). Uranyl ion species in the medium may interact with the adsorbents through electrostatics and complexation; therefore, the solution's ionic strength significantly affects these interactions. For the adsorption of uranium (VI) ions using cellulose-NH₂ and cellulose-COOH beads, the interactions between uranium (VI) and adsorbents are mainly electrostatic attractions. With the increasing ionic strength, the electrostatic interactions decrease between uranium (VI) ions and polycationic or polyanionic adsorbents due to the shielding effect. The adsorption efficiency of the cellulose-OH, cellulose-NH₂, and cellulose-COOH beads in

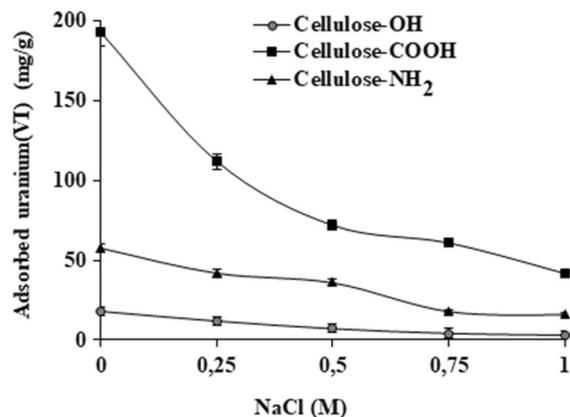


Fig. 6 Ionic strength of uranium (VI) adsorption on the cellulose-OH, cellulose-NH₂ and cellulose-COOH. (Initial uranium (VI) concentration, 100 mg/L; temperature, 25 °C; contact time, 120 min; stirring rate, 150 rpm)

NaCl free solution was 18.1 ± 0.3 , 59.4 ± 2.7 , and 192.6 ± 9.6 mg/g. In the presence of 1.0 mol/L NaCl, the adsorbed amount of uranium (VI) was found to be 3.1, 16.0, and 42.3 mg/g, respectively. As observed from Fig. 6, cellulose-COOH beads are more sensitive to NaCl concentration than cellulose-OH and cellulose-NH₂ beads. In the presence of NaCl in the medium, Na⁺ and Cl⁻ ions can shade the charged regions of the adsorbents, and the electrical bilayers of both adsorbents can be compressed, resulting in a reduction in electrostatic interactions and adsorbed uranium (VI). Similar findings have been reported in previous studies; for example, Ismaiel et al. (2022) studied the removal of Cu²⁺ in a solution using MgO adsorbent and reported that the electrostatic attraction reduced with an increasing salt concentration in the medium.

The effect of pH on the adsorption performance of the cellulose-NH₂ and cellulose-COOH beads

As observed from Fig. 7, the change in the pH of the solution led to either an increase or decrease in the adsorption performance of both adsorbents. The influence of pH on the adsorption performance of the cellulose-NH₂ and cellulose-COOH beads for uranyl ions was studied from the aqueous solution in the pH range of 3.0–8.0 (Fig. 7). The maximum amounts of uranium (VI) adsorption on the cellulose-NH₂ and cellulose-COOH beads were detected at pH 6.0,

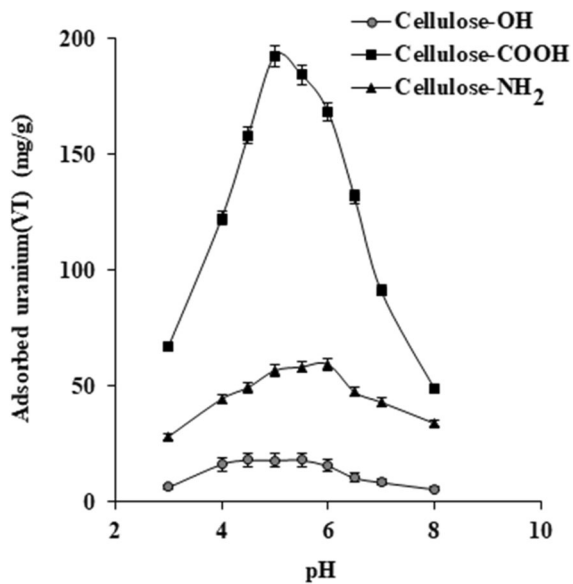


Fig. 7 Effect of pH on uranium (VI) adsorption on the cellulose-OH, cellulose-NH₂ and cellulose-COOH. (Adsorbent dose, 1.0 g/L; initial concentration of the uranium (VI), 100 mg/L; temperature, 25 °C; contact time, 120 min; stirring rate, 150 rpm)

and pH 5.0 as the optimal pH, respectively. As the medium pH value increased from 3.0 to 6.0 and 3.0 to 5.0 the adsorption capacities of the cellulose-NH₂ and cellulose-COOH beads for uranium (VI) ions were increased, respectively (Fig. 7). On the other hand, the removal performance of the cellulose-NH₂ and cellulose-COOH beads was decreased meaningfully with the increase of medium pH from 6.0 to 8.0 and from 5.0 to 8.0, respectively. At pH 6.0 and 5.0, the maximum adsorption capacities of the cellulose-NH₂ and cellulose-COOH beads were found to be 59.4 ± 2.7 and 192.6 ± 9.6 for uranium (VI) ions, respectively. As reported earlier, the pH is up to 5.0, the main forms of uranyl ions are UO_2^{2+} , UO_2OH^+ , and $(\text{UO}_2)_2(\text{OH})_2^{2+}$. At pH above 5.0, uranyl ions were present in the forms of $\text{UO}_2(\text{OH})_2\text{H}_2\text{O}$, $\text{UO}_2(\text{OH})^{3-}$, and $\text{UO}_2(\text{OH})_4^{2-}$ (Kanjilal et al. 2021; He et al. 2022). Therefore, a high amount of uranyl ion adsorbed on the cellulose-COOH beads at pH 5.0 compared to the other pH values studied. When the solution pH value was less than 5.0, the carboxyl group protonated, and a decrease in the amount of adsorbed uranyl ion was observed. Because uranium (VI) is a hard Lewis acid and interacts with hard Lewis bases such as oxygen-rich ligands. The $\text{N}\alpha, \text{N}\alpha$ -bis(carboxymethyl)-L-lysine

ligand has six oxygen atoms (three carboxyl groups). TEPA has only five amine groups that provide chelating sites for uranyl (VI) ions. From these results, the binding interaction of uranium (VI) ions on the cellulose-NH₂ and cellulose-COOH beads can primarily be considered a coordination complex formation, ion-exchange interaction, and physical forces.

In the pH range of 2.0–11.0, the zeta potential values of the cellulose-NH₂ were positive, meaning the surface of the adsorbent had positive charges. Thus, it generated an electrostatic repulsion between UO_2^{+2} ions in the medium and the cellulose-NH₂ beads, and the charge density in the pH ranges studied changed from 35.1 to 55.2 mV. On the other hand, the charge densities of the cellulose-COOH beads between pH 2.0 and 11.0 were negative and varied between -22.4 and -57.5 mV. Thus, cellulose-COOH beads can interact with positively charged uranyl ions and strongly adsorb on the negatively charged adsorbent. At a pH higher than 5.0, uranium ions hydrolyze into negatively charged uranyl species. The positively charged uranyl ion species may gradually decrease as the medium pH increases, and then, electrostatic attractions between TEPA ligand and uranium ions may increase. Therefore, an increase in the adsorption performance of the cellulose-NH₂ beads was observed at pH 6.0.

Influence of initial concentration and isotherms

From Fig. 8, when the initial concentration of uranium (VI) ions was increased from 10 to 300 mg/L in the medium, the amount of adsorbed uranium (VI) ions on both adsorbents increased until they reached equilibrium adsorption capacity. This may be because there are sufficient available adsorption sites for uranyl ions on the adsorbent at the lower initial concentration. Meanwhile, as the concentration of uranyl ions increased in the medium, the binding sites of the adsorbents gradually saturated and reached an equilibrium value. The equilibrium experimental adsorption capacities of the cellulose-OH, cellulose-NH₂, and cellulose-COOH beads were 25.1 ± 0.8 , 127.4 ± 5.1 and 462.9 ± 13.7 mg/g, respectively (Fig. 8). The uranium (VI) ions as a hard Lewis acid could easily interact with the hard Lewis bases such as oxygen-containing ligands. According to the Lewis acid–base theory, uranium (VI) ions tend to chelate and coordinate with

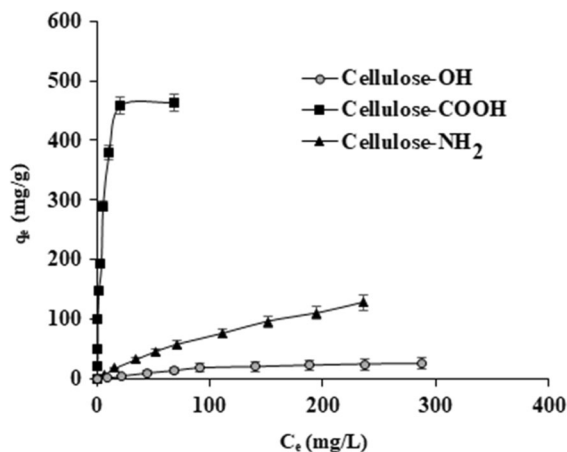


Fig. 8 Effect of initial concentration of uranium (VI) on adsorption capacity of cellulose-OH, cellulose-NH₂ and cellulose-COOH beads. (Adsorbent dose, 1.25 g/L; temperature, 25 °C; stirring rate, 150 rpm)

oxygen-containing ligands to form stable coordination bonds (Giannakoudakis et al. 2021). According to this theory, the oxygen atoms in the carboxyl groups of the cellulose-COOH beads chelated with the uranium (VI) ions. Meanwhile, the adsorption capacity of the cellulose-COOH beads was more than 3.5-fold more significant than that of the cellulose-NH₂ beads, demonstrating that the carboxyl groups of the adsorbent significantly increased its adsorption capacity. Moreover, at pH 5.0, the maximum uranium (VI) ions adsorption was observed; at this pH value, the carboxyl groups of the cellulose beads were deprotonated, and the surface of the beads displayed negative charges. The negatively charged adsorbent could lead to the high adsorption capacity for the predominant positively charged uranium (VI) ions. On the other hand, the uranium (VI) ions may mainly interact via chelate formation with the cellulose-NH₂ beads. From these results, the order of the adsorption capacity of the tested adsorbents used in uranium (VI) ion adsorption was cellulose-COOH > cellulose-NH₂ > cellulose-OH. It should be noted that the specific surface areas of the cellulose-OH, cellulose-NH₂, and cellulose-COOH were determined and found to be 20.7, 17.8, and 19.1 m²/g, respectively. These values were in the same order of magnitude. Thus, no relationship was observed between the adsorption capacities of the

adsorbents and the surface areas of the counterpart beads.

The adsorption of uranium (VI) ions on the cellulose-COOH and cellulose-NH₂ is studied using different adsorption isotherm models (i.e., Langmuir, Freundlich, and Temkin) to describe experimental data. The equation for the Langmuir adsorption isotherm model (Langmuir 1918).

$$q_e = q_m C_e / (K_d + C_e) \quad (2)$$

The Freundlich adsorption isotherm equation (Freundlich 1907):

$$q_e = K_F (C_e)^{1/n} \quad (3)$$

The Temkin isotherm model equation (Temkin and Pyzhev 1940):

$$q_e = q_T \ln K_T + q_T \ln C_e \quad (4)$$

The Langmuir plots were realized for the adsorption of uranium (VI) ions using the cellulose-NH₂ and cellulose-COOH beads, and the values of R² were in the range of 0.914–0.939 and 0.998–0.993, respectively (Table 2). From this table, the determined theoretical values of q_m for the cellulose-COOH beads agreed with the experimentally achieved adsorption capacities (q_{exp}), but the q_m values calculated for the cellulose-NH₂ were quite different from the experimental results. Therefore, the Langmuir model could not explain the adsorption of uranium (VI) ions on the cellulose-NH₂ beads.

Experimental values obtained for the adsorption of uranium (VI) ions on the cellulose-NH₂ and cellulose-COOH beads were plotted according to the Freundlich isotherm model, the model parameters such as n and K_F and the correlation coefficients (R²) were determined (Table 2). Analysis of the correlation coefficients, R², at different temperatures, indicated that the adsorption process better fits the Freundlich isotherm for the cellulose-NH₂. The major limitation of the Freundlich equation is that the maximum adsorption capacity cannot be evaluated. The K_F value is not a measure of total adsorption capacity but can be reflected as a proportional quantity of adsorption under certain conditions.

The Temkin isotherm parameters for the cellulose-NH₂ and cellulose-COOH beads, K_T means the equilibrium binding constant corresponding to the maximum binding energy at different temperatures

Table 2 Langmuir, and Freundlich isotherm model constants and correlation coefficients for U(VI) adsorption onto cellulose-NH₂ and cellulose-COOH beads

	T (K)	q (mg/g)	Langmuir constant			Freundlich constant		
			q _m (mg/g)	K _a × 10 ⁻⁴ (M ⁻¹)	R ²	n(L/mg)	K _F (mg/g)	R ²
Cellulose-NH ₂	288	110.8 ± 4.8	208.7	0.102	0.914	1.26	1.49	0.996
	298	127.4 ± 5.1	232.5	0.113	0.921	1.27	1.85	0.994
	308	130.3 ± 6.7	236.4	0.115	0.939	1.29	1.92	0.991
	318	134.1 ± 6.4	241.5	0.118	0.927	1.18	2.02	0.989
Cellulose-COOH	288	428.6 ± 18.9	534.4	1.38	0.997	1.54	35.7	0.860
	298	462.9 ± 13.7	468.2	7.76	0.998	2.09	100.1	0.916
	308	473.3 ± 21.7	494.9	21.9	0.993	2.32	127.0	0.808
	318	487.1 ± 19.6	491.8	49.4	0.997	3.03	210.7	0.723

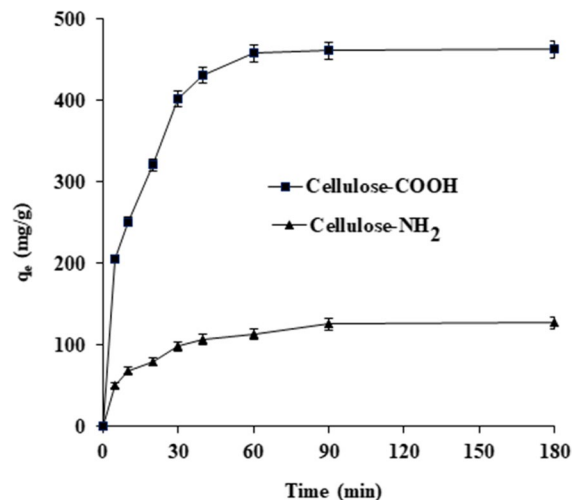
Table 3 Temkin isotherm model constants and correlation coefficients for U(VI) adsorption onto cellulose-NH₂ and cellulose-COOH beads

	Temkin constant				
	T (K)	Q _T (L/g)	b (kJ/mol)	K _T (mg/L)	R ²
Cellulose-NH ₂	288	39.3	14.5	0.103	0.955
	298	35.4	16.7	0.111	0.959
	308	33.6	18.1	0.126	0.961
	318	31.2	20.2	0.134	0.967
Cellulose-COOH	288	81.5	6.99	1.19	0.973
	298	77.2	7.63	7.82	0.954
	308	71.4	8.54	10.8	0.966
	318	65.9	9.55	85.7	0.979

and was ranging between 0.103 and 0.134, and 1.19 and 85.7 mg/L, respectively (Table 3). As a result, the Temkin model appears to propose the adsorption of uranium (VI) ions from the solution on the cellulose-COOH beads. Meanwhile, the model fits the adsorption of uranium ions on the cellulose-NH₂.

Adsorption kinetic studies

As seen from Fig. 9, the adsorption equilibrium time of the uranium ions at 300 mg/L initial concentration from aqueous solution with the cellulose-NH₂ and cellulose-COOH beads was reached within 90 min. The observed change in the adsorption equilibrium was very fast in the early stage, up to 60 min, and gradually reached equilibrium adsorption within

**Fig. 9** Effect of contact time on adsorption of uranium (VI) on the cellulose-OH, cellulose-NH₂ and cellulose-COOH beads, (Adsorbent dose, 1.25 g/L; temperature, 25 °C; stirring rate, 150 rpm)

90 min. At the initial phase of adsorption, the empty binding sites were progressively occupied, then the adsorption rate of uranium (VI) ions slowed down and reached equilibrium.

The pseudo-first- and pseudo-second order kinetics were studied to evaluate the adsorption mechanism of the cellulose-NH₂ and cellulose-COOH beads. In literature, the adsorption kinetics of uranium (VI) ions were obtained with different adsorbents. These results showed a wide range of adsorption rates (Hu et al. 2021; Deng et al. 2021). In the presented study,

a rapid adsorption rate was obtained for both adsorbents for approximately 90 min.

The adsorption kinetics of the adsorbents are examined by using the experimental data achieved by the adsorption of uranium (VI) ions from aqueous solutions on the cellulose-NH₂ and cellulose-COOH beads. The first-order kinetic model equation (Lagergren 1898):

$$dq_t/dt = k_1(q_e - q_t) \quad (5)$$

$$\log(q_e - q_t) = \log q_e - (k_1 \cdot t)/2.303 \quad (6)$$

The linear form of the second-order equation (Ho, and McKay 1999):

$$t/q_t = 1/(k_2 q_e^2)t + 1/q_e \quad (7)$$

It can be seen that R² values for the second-order equation were in the range of 0.989–0.999 for the tested adsorbents. On the other hand, the first-order equation R² values fall in the range of 0.869–0.944, respectively. These results show that the adsorption process fits better into the second-order equation (Table 4). Additionally, the calculated adsorption capacities (q_e) achieved from the second-order kinetic equation for the uranium (VI) ions using both tested adsorbents were in agreement with the experimental values (q_{exp}). The values of theoretical equilibrium adsorption capacities (q_e) increased for the cellulose-NH₂ and cellulose-COOH beads from 117.3 to 137.69 mg/g and from 457.9 to 501.5 mg/g as the temperatures increased from 288 to 318 K, respectively (Table 4).

Influence of temperature and thermodynamics parameters

The effect of temperature on the removal of uranium (VI) ions using the cellulose-NH₂ and cellulose-COOH beads at different temperatures is presented in Table 4. The adsorption performance of both adsorbents increased with increasing temperature. The increasing temperature may provide an enhancement in the surface area of adsorbents and the collision rates of uranium (VI) ions with binding sites. Thus, these parameters could influence the amount of adsorbed uranium (VI) ions. From Table 4, the adsorbed amount of uranium (VI) ions was seriously temperature dependent. This displayed that uranium (VI) adsorption on cellulose-NH₂ and cellulose-COOH beads was quite favorable at high temperatures, and the adsorption process on both tested adsorbents may be endothermic.

The Gibbs free energy change (ΔG°) of adsorption uranium on the adsorbents was determined from the following equation:

$$\Delta G = -RT \ln K_a \quad (8)$$

Standard enthalpy (ΔH) and entropy change (ΔS) values of adsorption of uranium (VI) on the adsorbents are determined from van't Hoff equation:

$$\ln K_a = -\Delta H/RT + \Delta S/R \quad (9)$$

The values of ΔH and ΔS were determined from the slope and intercept from the drawn curve of lnK_a versus 1/T, respectively. Negative ΔG values were obtained for both adsorbents, showing that the adsorption process

Table 4 First and second-order kinetic constants for U(VI) adsorption onto cellulose-NH₂ and cellulose-COOH beads

	T (K)	q _{exp} (mg/g)	First-order			Second-order			h (mg/g min)
			q _{eq} (mg/g)	k ₁ × 10 ² (min ⁻¹)	R ²	q _{eq} (mg/g)	k ₂ × 10 ⁴ (g/mg/min)	R ²	
Cellulose-NH ₂	288	110.8 ± 4.8	142.5	6.36	0.919	117.3	9.7	0.999	13.3
	298	127.4 ± 5.1	234.3	7.27	0.934	136.2	7.0	0.989	13.0
	308	130.3 ± 6.7	479.4	11.4	0.920	135.8	10.9	0.996	20.1
	318	134.1 ± 6.4	197.7	9.53	0.904	137.6	19.9	0.999	37.7
Cellulose-COOH	288	428.6 ± 18.9	753.1	6.63	0.869	457.9	1.9	0.996	39.8
	298	462.9 ± 13.7	523.3	7.48	0.944	487.1	2.9	0.999	70.0
	308	473.3 ± 21.7	609.5	8.73	0.914	493.6	3.6	0.998	87.2
	318	487.1 ± 19.6	940.7	10.3	0.935	501.5	4.6	0.997	114.7

of uranium (VI) ions was spontaneous (Table 5). In this study, the ΔG values were in the range of -16.6 and -18.7 for cellulose-NH₂ and -22.8 and -34.7 kJ/mol for the cellulose-COOH beads. These data showed that uranium (VI) adsorption on cellulose-NH₂ and cellulose-COOH beads was physical and combined physical/chemical, respectively. The positive ΔS values showed that uranium (VI) ions had a high affinity to the adsorbents. The positive value of ΔH° (3.38 for the cellulose-NH₂ and 30.1 kJ/mol for the cellulose-COOH beads) suggested that the adsorption of uranium (VI) was endothermic and spontaneous on both adsorbents (Table 5).

Adsorption mechanisms

Electrostatic and ion-exchange interactions may explain the adsorption of uranyl ions by the cellulose-NH₂ and cellulose-COOH beads. As specified in the FTIR spectra, the -OH and -NH₂ functional groups were observed at around 3500 and 3250 cm⁻¹. These groups are accountable for the electrostatic interactions and can affect the adsorption capacities of the cellulose-NH₂ beads. Furthermore, the vibration of the amide I band was seen at 1649 cm⁻¹, and the peak at 1582 cm⁻¹ could be donated as the -NH bending of the amide II band. Therefore, the presence of these groups on the cellulose-NH₂ beads may provide interaction with uranium (VI) ions via coordination complexation or electrostatic interactions. For cellulose-COOH beads, the peaks observed at 1725 cm⁻¹ (C=O) and 1397 cm⁻¹ stretching vibration and the symmetric stretching vibration of COO⁻ indicated the role of carboxyl groups in uranium (VI) adsorption.

Table 5 Thermodynamic parameters for U(VI) adsorption onto cellulose-NH₂ and cellulose-COOH beads

Adsorbent	T (K)	ΔG (kJ/mol)	ΔH (kJ/mol)	ΔS (kJ/mol K)	E_a (kJ/mol)
Cellulose-NH ₂	288	-16.6	3.38	0.068	19.4
	298	-17.4			
	308	-18.0			
	318	-18.7			
Cellulose-COOH	288	-22.8	30.1	0.379	24.5
	298	-27.9			
	308	-30.9			
	318	-34.7			

These results suggested that the oxygen atoms of carboxyl groups (C=O or C-O) in the cellulose-COOH structure played an essential role in detecting high uranium (VI) adsorption.

Desorption and regeneration studies

Adsorption/desorption studies were performed to test the cyclic usability of the adsorbents. Therefore, the uranium (VI) loaded cellulose-NH₂ and/or cellulose-COOH beads were desorbed with a low concentration of HNO₃ (20 mmol/L) solution as described previously (Celikbicak et al. 2021). Thus, the regenerated both modified cellulose-based adsorbents were used for the repeated uranium (VI) ion adsorption. The adsorption/desorption studies were repeated seven times using the same tested adsorbents. The experimental data are presented in Table S1. It was observed that after seven cycles, the adsorption capacity of the cellulose-NH₂ beads for uranium (VI) decreased by about 13.0% and retained the initial adsorption capacity of about 87%. On the other hand, under the same conditions, cellulose-COOH beads lost their initial adsorption capacity of about 7.3%. These results show that both adsorbents have high reusability and regeneration potential. Thus, they could be used as commercial and environmentally approachable adsorbents to remove various metals from solutions.

Comparison of prepared adsorbent with previously reported studies

It is necessary to compare the adsorption performance of newly developed adsorbents with existing adsorbents for environmental applications (Table 6). As can be seen from this table, the adsorption capacities of the cellulose-NH₂ and cellulose-COOH beads for the U(VI) ions could be compared to the previously reported studies (Ahmed et al. 2021, Bi et al. 2021, Ashrafi and Firouzzare 2021, Bayramoglu and Arica 2017, Liu et al. 2022, Zhang et al. 2023, He et al. 2022, Kanjilal et al. 2021, Liu et al. 2021, Wang et al. 2020 and Orabi et al. 2021). The prepared adsorbents had comparable adsorption performance with the earlier reports. The obtained high adsorption capacities could be due to the presence of polycarboxyl and polyamine groups and the interaction of these groups with the uranium (VI) ion through electrostatic, ion exchange interactions and coordination complex. As stated above, the cellulose-COOH beads were more satisfactory for removing uranium U(VI) ions

Table 6 Comparison of the adsorption capacities of adsorbents for U(VI)

The adsorbent	Q_{max} (mg/g)	References
Biochar/ Hydroxyapatite-biochar	110.6/428.3	(Ahmed et al. 2021)
Zr-MOF on functionalized graphene oxide	436.0	(Bi et al. 2021)
Polyacrylonitrile-graphene oxide	345.1	(Ashrafi and Firouzzare 2021)
Poly(GMA-EGDMA) beads modified with polyethylene imine and tris(2-aminoethyl) amine groups	87.8/64.3	(Bayramoglu and Arica 2017)
Polyethylenimine-activated carbon	50.3	(Liu et al. 2022)
Polyamidoxime magnetic chitosan beads	5.1	(Zhang et al. 2023)
Phosphonic acid-aromatic based porous polymer	222.7	(He et al. 2022)
Phosphonic acid functionalized aromatic-based porous	222.7	(Kanjilal et al. 2021)
Chitosan grafted titanium dioxide	163.2	(Wang et al. 2020)
Polysulfone-chitosan grafted p-phenylenediamine/Cellulose acetate-chitosan grafted p-phenylenediamine	44/39	(Orabi et al. 2021)
Sulfhydryl-functionalized biomass carbon supported nano-zero-valent iron	273.0	(Liu et al. 2021)
Cellulose-NH ₂ / Cellulose-NH ₂	127.4/462.9	(In this work)

compared to the cellulose-NH₂ beads from the solution. The high adsorption performance of the carboxyl groups for uranium (VI) ions may result from the ion-exchange interaction of this group with uranyl ions.

Conclusion

In this work, polycationic (cellulose-NH₂) and polyanionic (cellulose-COOH) cellulose beads for the removal of uranium (VI) were prepared. These adsorbents were characterized by FTIR, SEM, zeta potential analysis, and analytical methods for validation of modification with different functional groups. FTIR studies confirmed the presence of amine (R-NH₂) and carboxylic (R-COOH) groups on the cellulose beads. The maximum experimental adsorption capacities of the cellulose-NH₂ (at pH 6.0) and cellulose-COOH (at pH 5.0) were found to be 127.4 and 462.9 mg/g, at 25 °C, respectively. Uranium (VI) is considered a hard Lewis acid and, as expected, showed ion-exchange performance for uranyl ions. Therefore, a high adsorption capacity was obtained with cellulose-COOH beads for uranium (VI) ions compared to cellulose-NH₂ beads. The adsorption behavior of cellulose-NH₂ can be described with Freundlich isotherm and Temkin isotherm models, whereas the adsorption of uranium (VI) on the cellulose-COOH adsorbent well fitted the Langmuir isotherm model. The adsorption of uranium (VI) on

both adsorbents was well described with the pseudo-second-order model. The thermodynamic parameter of uranium (VI) adsorption on the cellulose-NH₂ and cellulose-COOH beads displayed that the adsorption process was spontaneous. These results demonstrated that the cellulose-COOH beads have a high potential for effectively removing uranium (VI) ions from the aqueous solution. The cellulose-NH₂ and cellulose-COOH beads revealed good reusability during repeated adsorption/desorption cycles, and their adsorption capacities decreased by about 13.0 and 7.3% after seven cycles, respectively. Finally, the preparations of the presented adsorbents were simple, and especially cellulose-COOH has a high adsorption capacity. Both adsorbents are environmentally friendly and can be used for the adsorption of various inorganic and organic pollutants.

Author's contribution Gulay Bayramoglu: Visualization, Validation, Writing—original draft, Writing—review & editing. Serhat Tilki: Investigation. M. Yakup Arica: Formal analysis, Conceptualization, Writing—review & editing.

Funding Open access funding provided by the Scientific and Technological Research Council of Türkiye (TÜBİTAK).

Data availability All data and materials are true and valid and can use general repositories saving and also data are provided upon request.

Declarations

Ethics approval Not applicable.

Consent to participate Not applicable.

Consent for publication All authors have given consent for publication.

Competing interests The authors declare no competing interests.

Open Access This article is licensed under a Creative Commons Attribution 4.0 International License, which permits use, sharing, adaptation, distribution and reproduction in any medium or format, as long as you give appropriate credit to the original author(s) and the source, provide a link to the Creative Commons licence, and indicate if changes were made. The images or other third party material in this article are included in the article's Creative Commons licence, unless indicated otherwise in a credit line to the material. If material is not included in the article's Creative Commons licence and your intended use is not permitted by statutory regulation or exceeds the permitted use, you will need to obtain permission directly from the copyright holder. To view a copy of this licence, visit <http://creativecommons.org/licenses/by/4.0/>.

References

- Ahmed W, Núñez-Delgado A, Mehmood S, Qaswar SAM, Shaikoor A, Chen D-Y (2021) Highly efficient uranium (VI) capture from aqueous solution by means of a hydroxyapatite-biochar nanocomposite: Adsorption behavior and mechanism. *Environ Res* 201:111518. <https://doi.org/10.1016/j.envres.2021.111518>
- Arica MY, Bayramoglu G (2016) Polyaniline coated magnetic carboxymethylcellulose beads for selective removal of uranium ions from aqueous solution. *J Radioanal Nucl Chem* 310:711–724. <https://doi.org/10.1007/s10967-016-4828-z>
- Arica TA, Balci FM, Balci S, Arica MY (2022) Highly porous poly (o-phenylenediamine) loaded magnetic carboxymethyl cellulose hybrid beads for removal of two model textile dyes. *Fiber Polym* 23:2838–2854. <https://doi.org/10.1007/s12221-022-0221-4>
- Ashrafi F, Firouzzare M (2021) Preparation of forcespun amidoximated polyacrylonitrile-graphene oxide nanofibers and evaluation of their uranium uptake from aqueous media. *Fiber Polym* 22:3289–3297. <https://doi.org/10.1007/s12221-021-0133-8>
- Bai J, Li S, Ma X, Yan H, Su S, Wang S, Wang J (2022) Novel preparation of amidoxime functionalized hyper-cross-linked polymeric adsorbent on the efficient adsorption of uranium in aqueous solution. *Micropor Mesopor Mater* 331:111647. <https://doi.org/10.1016/j.micromeso.2021.111647>
- Bayramoglu G, Arica MY (2017) Polyethylenimine and tris(2-aminoethyl)amine modified p(GA–EGMA) microbeads for sorption of uranium ions: equilibrium, kinetic and thermodynamic studies. *J Radioanal Nucl Chem* 312:293–303. <https://doi.org/10.1007/s10967-017-5216-z>
- Bayramoglu G, Arica MY (2019) Star type polymer grafted and polyamidoxime modified silica coated-magnetic particles for adsorption of U(VI) ions from solution. *Chem Eng Res Des* 147:146–159. <https://doi.org/10.1016/j.cherd.2019.04.039>
- Bayramoglu G, Akbulut A, Arica MY (2015) Study of polyethyleneimine- and amidoxime-functionalized hybrid biomass of *Spirulina (Arthrospira) platensis* for adsorption of uranium (VI) ion. *Environ Sci Pollut Res* 22:17998–18010. <https://doi.org/10.1007/s11356-015-4990-9>
- Bayramoglu G, Akbulut A, Acikgoz-Erkaya I, Arica MY (2018) Uranium sorption by native and nitrilotriacetate-modified *Bangia atropurpurea* biomass: kinetics and thermodynamics. *J Appl Phycol* 30:649–661. <https://doi.org/10.1007/s10811-017-1238-8>
- Bayramoglu G, Kilic M, Arica MY (2023) *Trametes trogii* biomass in carboxymethylcellulose-lignin composite beads for adsorption and biodegradation of bisphenol A. *Biodegradation* 34:263–281. <https://doi.org/10.1007/s10532-023-10024-7>
- Bi C, Zhang C, Ma F, Zhang X, Yang M, Nian J, Liu L, Dong H, Zhu L, Wang Q, Guo S, Lv Q (2021) Growth of a mesoporous Zr-MOF on functionalized graphene oxide as an efficient adsorbent for recovering uranium (VI) from wastewater. *Micropor Mesopor Mater* 323:111223. <https://doi.org/10.1016/j.micromeso.2021.111223>
- Brunauer S, Emmett PH, Teller E (1938) Adsorption of gases in multimolecular layers. *J Am Chem Soc* 60:309–319. <https://doi.org/10.1021/ja01269a023>
- Celikbıçak O, Bayramoglu G, Acikgoz-Erkaya I, Arica MY (2021) Aggrandizement of uranium (VI) removal performance of *Lentinus concinnus* biomass by attachment of 2,5-diaminobenzenesulfonic acid ligand. *J Radioanal Nucl Chem* 328:1085–1098. <https://doi.org/10.1007/s10967-021-07708-w>
- Chen L, Wang Y, Cao X, Zhang Z, Liu Y (2023) Effect of doping cation on the adsorption properties of hydroxyapatite to uranium. *J Solid State Chem* 317:123687. <https://doi.org/10.1016/j.jssc.2022.123687>
- Cheng Y, Li F, Liu N, Lan T, Yang Y, Zhang T, Liao J, Qing R (2021) A novel freeze-dried natural microalga powder for highly efficient removal of uranium from wastewater. *Chemosphere* 282:131084. <https://doi.org/10.1016/j.chemosphere.2021.131084>
- Deng M, Ai Y, Zhao L, Xu Y, Ouyang Y, Yang P, Peng G (2021) Preparation of NH₂-CTS/MZ composites and their adsorption behavior and mechanism on uranium ions. *J Radioanal Nucl Chem* 330:963–978. <https://doi.org/10.1007/s10967-021-07991-7>
- Edwards JV, Prevost NT, Condon B, French A, Wu Q (2012) Immobilization of lysozyme-cellulose amide-linked conjugates on cellulose I and II cotton nanocrystalline preparations. *Cellulose* 19:495–506. <https://doi.org/10.1007/s10570-011-9637-5>
- Fan M, Wang X, Song Q, Zhang L, Ren B, Yang X (2021) Review of biomass-based materials for uranium adsorption. *J Radioanal Nucl Chem* 330:589–602. <https://doi.org/10.1007/s10967-021-08003-4>

- French AD (2017) Glucose, not cellobiose, is the repeating unit of cellulose and why that is important. *Cellulose* 24:4605–4609. <https://doi.org/10.1007/s10570-017-1450-3>
- Freundlich H (1907) Über die Adsorption in Lösungen. *Z Phys Chem Stöchiometrie Verwandtschaftslehre* 57(4):385–470
- Gericke M, Trygg J, Fardim P (2013) Functional cellulose ceads: Preparation, characterization, and applications. *Chem Rev* 113:4812–4836. <https://doi.org/10.1021/cr300242j>
- Giannakoudakis DA, Anastopoulos I, Barczak M, Antoniou E, Terpilowski K, Mohammadi E, Shams M, Coy E, Bakandritsos A, Katsoyiannis IA, Colmenares JC, Pashalidis I (2021) Enhanced uranium removal from acidic wastewater by phosphate-functionalized ordered mesoporous silica: Surface chemistry matters the most. *J Hazard Mater* 413:125279. <https://doi.org/10.1016/j.jhazmat.2021.125279>
- Hamza MF, Wei Y, Khalafalla MS, Abed NS, Fouda A, Elwakeel KZ, Guibal E, Hamadh NA (2022) U(VI) and Th(IV) recovery using silica beads functionalized with urea- or thiourea-based polymers – Application to ore leachate. *Sci Total Environ* 821:153184. <https://doi.org/10.1016/j.scitotenv.2022.153184>
- Hana J, Zhou C, French AD, Han G, Wu Q (2013) Characterization of cellulose II nanoparticles regenerated from 1-butyl-3-methylimidazolium chloride. *Carbohydr Polym* 94:773–781. <https://doi.org/10.1016/j.carbpol.2013.02.003>
- He Y, Bao W, Li B, Fu X, Na B, Yuan D (2022) Highly efficient removal of uranium from aqueous solution by a novel robust phosphonic acid functionalized aromatic-based hyper-crosslinked porous polymer. *J Radioanal Nucl Chem* 331:3745–3756. <https://doi.org/10.1007/s10967-022-08395-x>
- Ho YS, McKay G (1999) Pseudo-second-order model for sorption processes. *Process Biochem* 34:451–465
- Hu B, Wang H, Liu R, Qiu M (2021) Highly efficient U(VI) capture by amidoxime/carbon nitride composites: Evidence of EXAFS and modeling. *Chemosphere* 274:129743. <https://doi.org/10.1016/j.chemosphere.2021.129743>
- Huang Z, Wu P, Yin Y, Wang S, Zhang J, Guo Z, Hayat T, Alharbi NS, Heet C (2021) Preparation of cotton fibers modified with aromatic heterocyclic compounds and study of Cr(VI) adsorption performance. *Cellulose* 28:11037–11049. <https://doi.org/10.1007/s10570-021-04217-7>
- Ismail MMS, El-Ayouty YM, Abdelaal SA, Fathey HA (2022) Biosorption of uranium by immobilized *Nostoc sp.* and *Scenedesmus sp.*: kinetic and equilibrium modeling. *Environ Sci Pollut Res* 29:83860–83877. <https://doi.org/10.1007/s11356-022-21641-9>
- Kanjilal A, Singh KK, Tyagi AK, Dey GR (2021) Synthesis of bi-functional chelating sorbent for recovery of uranium from aqueous solution: sorption, kinetics and reusability studies. *J Polym Res* 28:460. <https://doi.org/10.1007/s10965-021-02819-0>
- Lagergren S (1898) Zur theorie der sogenannten Adsorption gel oster stoffe. *Kungliga Svenska Vetenskapsakademiens Handlingar* 25(4):1–39
- Langmuir I (1918) The adsorption of gases on plane surfaces of glass, mica and platinum. *J Am Chem Soc* 40:1361–1403
- Liu X, Liu Y, Wang Y, Yuan D, Wang C, Liu J (2021) Efficient electro-sorption of uranium(VI) by B, N, and P co-doped porous carbon materials containing phosphate functional groups. *J Solid State Electrochem* 25:2443–2454. <https://doi.org/10.1007/s10008-021-05029-2>
- Liu C, Lu J, Tan Y, Chen B, Yang P (2022) Removal of U(VI) from wastewater by sulfhydryl-functionalized biomass carbon supported nano-zero-valent iron through synergistic effect of adsorption and reduction. *Mater Sci Eng B* 284:115891. <https://doi.org/10.1016/j.mseb.2022.115891>
- Minrui O, Wanying L, Zhang Z, Xu X (2022) β -Cyclodextrin and diatomite immobilized in sodium alginate biosorbent for selective uranium (VI) adsorption in aqueous solution. *Int J Biol Macromol* 222:2006–2016. <https://doi.org/10.1016/j.ijbiomac.2022.09.290>
- Orabi AH, Abdelhamid AE, Salem HM, Ismaiel DA (2021) Uranium removal using composite membranes incorporated with chitosan grafted phenylenediamine from liquid waste solution. *Cellulose* 28:3703–3721. <https://doi.org/10.1007/s10570-021-03749-2>
- Peng T-Q, Wang Y-F, Xu Y-F, Liu Z-C (2023) Synthesis, characterization and uranium (VI) adsorption mechanism of novel adsorption material poly(tetraethylenepentamine–trimesoyl chloride). *J Radioanal Nucl Chem* 332:409–422. <https://doi.org/10.1007/s10967-022-08739-7>
- Shen J, Cao F, Liu S, Wang C, Chen R, Chen K (2022) Effective and selective adsorption of uranyl ions by porous polyethylenimine-functionalized carboxylated chitosan/oxidized activated charcoal composite. *Front Chem Sci Eng* 16:408–419. <https://doi.org/10.1007/s11705-021-2054-x>
- Singh S, Kaur M, Bajwa BS, Kaur I (2022) Salicylaldehyde and 3-hydroxybenzoic acid grafted NH₂-MCM-41: Synthesis, characterization and application as U(VI) scavenging adsorbents using batch mode, column and membrane systems. *J Mol Liq* 346:117061. <https://doi.org/10.1016/j.molliq.2021.117061>
- Smjencanin N, Buzo D, Masic D, Nuhanovic M, Sulejmanovic J, Azhar O, Sher F (2022) Algae based green biocomposites for uranium removal from wastewater: Kinetic, equilibrium and thermodynamic studies. *Mater Chem Phys* 283:125998
- Temkin MJ, Pyzhev V (1940) Application of temkin adsorption isotherm. *Acta Physiol Chem USSR* 12:271
- Wang J, Huo Y, Ai Y (2020) Experimental and theoretical studies of chitosan modified titanium dioxide composites for uranium and europium removal. *Cellulose* 27:7765–7777. <https://doi.org/10.1007/s10570-020-03337-w>
- WHO (2011) Uranium in drinking water. Background document for development of WHO guidelines for drinking water quality. WHO/SDE/WSH/03.04/118/Rev/1, Geneva
- Xiao F, Cheng Y, Zhou P, Chen S, Wang X, He P, Nie X, Dong F (2021) Fabrication of novel carboxyl and amidoxime groups modified luffa fiber for highly efficient removal of uranium(VI) from uranium mine water. *J Environ Chem Eng* 9:105681. <https://doi.org/10.1016/j.jece.2021.105681>
- Zhang Y, Cai T, Zhao Z, Han B (2023) Poly(amidoxime)-graft-magnetic chitosan for highly efficient and selective uranium extraction from seawater. *Carbohydr Polym* 301:120367. <https://doi.org/10.1016/j.carbpol.2022.120367>
- Zhou S, Xie Y, Zhu F, Gao Y, Liu Y, Tang Z, Duan Y (2021) Amidoxime modified chitosan/graphene oxide composite for efficient adsorption of U(VI) from aqueous solutions. *J Environ Chem Eng* 9:106363. <https://doi.org/10.1016/j.jece.2021.106363>
- Zhu R, Zhang C, Bi C, Zhu L, Wang C, Wang Y, Liu L, Ma F, Dong H (2023) Highly efficient and antibacterial uranium

adsorbents derived from disubstituted amidoxime functionalized chitosan. *Cellulose* 30:1669–1684. <https://doi.org/10.1007/s10570-022-04996-7>

Zong P, Cao D, Cheng Y, Wang S, Zhang J, Guo Z, Hayat T, Alharbi NS, He C (2019) Carboxymethyl cellulose supported magnetic graphene oxide composites by plasma induced technique and their highly efficient removal of uranium ions. *Cellulose* 26:4039–4060. <https://doi.org/10.1007/s10570-019-02358-4>

Publisher's Note Springer Nature remains neutral with regard to jurisdictional claims in published maps and institutional affiliations.